

# Evaluating Polarizing Quantities for Quadrilateral Ground Distance Protection: Field Insights and Practical Guidelines

Kanchanrao Dase, Kale McCarthy, Muhammad Ashraf, and Armando Guzmán  
*Schweitzer Engineering Laboratories, Inc.*

Presented at the  
52nd Annual Western Protective Relay Conference  
Spokane, Washington  
October 28–30, 2025

# Evaluating Polarizing Quantities for Quadrilateral Ground Distance Protection: Field Insights and Practical Guidelines

Kanchanrao Dase, Kale McCarthy, Muhammad Ashraf, and Armando Guzmán,  
Schweitzer Engineering Laboratories, Inc.

**Abstract**—This paper explores the process of selecting polarizing quantities for the ground reactance element in quadrilateral distance protection. While the operating quantity of the reactance element for a given reach cannot be altered, most protective relays provide flexibility in selecting the polarizing quantity—typical options include loop, negative-sequence, or zero-sequence current. Negative-sequence current has been the traditional choice because of network homogeneity and the minimal impact from mutual coupling in parallel line applications. However, the growing integration of inverter-based resources with unreliable negative-sequence current sources has prompted a shift toward zero-sequence and loop current polarization. While there are concerns about mutual coupling in parallel lines, this paper shows that zero-sequence current remains a reliable option for polarization. The paper derives zero-sequence polarizing current tilt angle expressions for all typical parallel line configurations, demonstrating that the polarization angle depends on zero-sequence network parameters and not on the parallel line currents. The paper discusses that overreach and underreach issues are caused by the mutually coupled zero-sequence voltage across the protected line, rather than the choice of the polarizing current. The paper provides practical guidelines to select the appropriate polarizing quantity for the reactance element and validates the recommended guidelines with real-world case studies.

## I. INTRODUCTION

Traditionally, reactance elements have been used to protect power lines for phase-to-ground faults, aiming to detect faults with high fault resistance,  $R_F$ . The ground distance protective relays that incorporated these elements were initially electromechanical relays, such as the one described in [1], which continue to be in service today providing line protection. These relays feature a reactance unit that is supervised by a mho-type starting unit. Fig. 1 shows the operating characteristic of this reactance relay.

For the operating characteristic shown in Fig. 1, the reactance  $X_\varphi$  is calculated according to (1).

$$X_\varphi = \left| \frac{V_\varphi}{I_{\varphi\_COMP}} \right| \cdot \sin \theta \quad (1)$$

where:

$V_\varphi$  is the faulted phase-to-ground voltage.

$I_{\varphi\_COMP}$  is the phase current with zero-sequence current compensation as expressed in (2).

$\theta$  is the angle difference between  $V_\varphi$  and  $I_{\varphi\_COMP}$ .

$\varphi$  represents Phase A, B, or C.

$$I_{\varphi\_COMP} = I_\varphi + \left( \frac{X_{0L} - X_{1L}}{X_{1L}} \right) I_0 \quad (2)$$

where:

$I_0$  is the zero-sequence current that the relay measures.

$X_{1L}$  and  $X_{0L}$  are the positive-sequence and zero-sequence reactances of the line, respectively.

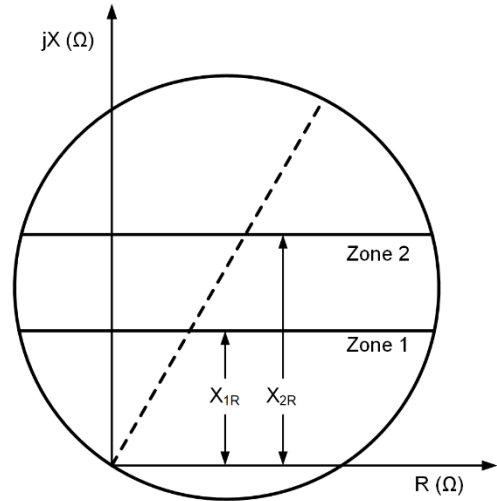


Fig. 1. Operating characteristics of the initial reactance relay [1].

While the starting unit is operated, the Zone 1 and Zone 2 relay outputs operate when  $X_\varphi$  is less than the reach settings  $X_{1R}$  and  $X_{2R}$  from Fig. 1, respectively.

The characteristic of the reactance relay shown in Fig. 1 was the predecessor to the development of quadrilateral characteristics. Early implementations of quadrilateral characteristics in static electronic protective relays used loop polarization for the reactance element [2]. Fig. 2 shows this characteristic with the corresponding resistive ( $R_{SET}$ ) and reactance ( $X_{SET}$ ) element settings. The reactance element characteristic shown in Fig. 1 and Fig. 2 is fixed in the impedance plane because the reactance element is polarized with loop current.

The use of negative-sequence polarization for the reactance element was proposed because the negative-sequence network is more homogeneous than the zero-sequence network and is less affected by mutual coupling in parallel line applications [3] [4] [5].

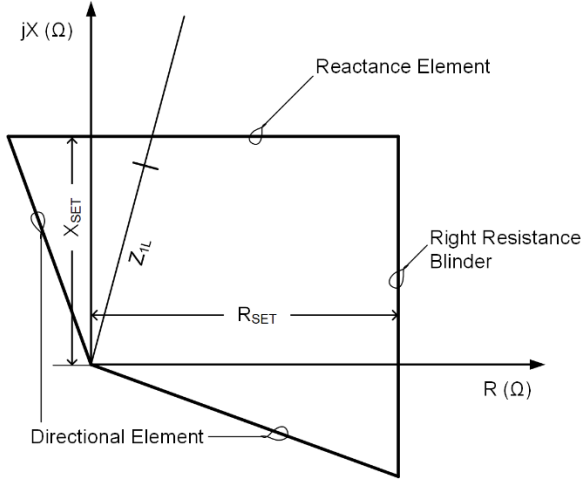


Fig. 2. Early quadrilateral characteristic in a static electronic protective relay.

Numerical relays do not have the constraints that electromechanical and static electronic protective relays have; they include quadrilateral characteristics that consist of a reactance element, right and left resistance blinders, and an associated directional element. The reactance element in these relays uses phase comparison to define its characteristic. The phase comparator measures the phase difference between an operating quantity ( $I_{\phi\text{LOOP}} \cdot Z_R - V_{\phi}$ ) and a polarizing quantity to determine whether the operating point is inside the characteristic. Here,  $Z_R$  is the reach impedance setting. This paper analyzes ground reactance elements polarized with loop, negative-sequence, or zero-sequence currents. Equation (3) is an expression of a phase comparator for the current-polarized ground reactance element calculation. Note that (1) can also be expressed using (3).

$$m \cdot |Z_{1L}| = \frac{\text{Im}[V_{\phi} \cdot (I_{\text{POL}} \cdot e^{jT})^*]}{\text{Im}[e^{j\theta_{L1}} \cdot I_{\phi\text{LOOP}} \cdot (I_{\text{POL}} \cdot e^{jT})^*]} \quad (3)$$

where:

$m$  is the pu impedance from the relay location to the fault.

$Z_{1L}$  is the positive-sequence line impedance.

$\theta_{L1}$  is the angle of the positive-sequence line impedance.

$I_{\phi\text{LOOP}}$  is the faulted-phase loop current.

$I_{\text{POL}}$  is the polarizing current.

$T$  is the tilt angle of the reactance element.

\* indicates a complex conjugate.

Equation (4) defines the zero-sequence compensation factor  $k_0$ , where  $Z_{0L}$  is the zero-sequence line impedance.

$$k_0 = \frac{Z_{0L} - Z_{1L}}{3 \cdot Z_{1L}} \quad (4)$$

Equation (5) defines  $I_{\phi\text{LOOP}}$ .

$$I_{\phi\text{LOOP}} = I_{\phi} + k_0 \cdot I_R \quad (5)$$

where  $I_R$  is the residual current, which is the sum of the phase currents ( $I_R = I_A + I_B + I_C$ ).

The evolving nature of power systems, driven by the increasing integration of inverter-based resources (IBRs), has introduced new challenges. IBRs often exhibit unreliable

negative-sequence current sources, which undermines the effectiveness of negative-sequence current as a polarizing quantity [6]. Consequently, zero-sequence and loop current polarizations are being used for these applications.

The use of zero-sequence current as a polarizing quantity raises concerns, especially in systems with parallel lines where zero-sequence mutual coupling is present. Utilities often question whether such coupling could compromise the reliability of the polarization and lead to misoperations of the distance element. This paper addresses these concerns by demonstrating that zero-sequence current polarization remains a viable and dependable option, even in the presence of mutual coupling in parallel line applications.

To support this claim, the paper derives analytical expressions for the required tilt angle of the zero-sequence current polarization across typical parallel line configurations. These expressions reveal that the polarization angle is governed by the parameters of the zero-sequence network and is unaffected by the current in adjacent lines. Furthermore, the study clarifies that the underreach or overreach issues associated with the reactance element are caused by mutually coupled zero-sequence voltage across the protected line, rather than the choice of polarizing current itself. These reach issues in parallel line configurations can be effectively addressed by applying an appropriate zero-sequence compensation factor or by adjusting the reach settings, as discussed in [7] and [8].

This paper focuses on reactance elements. However, mutual coupling in parallel line applications also affects the performance of ground directional elements that are polarized with zero-sequence current. The performance of these directional elements needs to be evaluated when zero-sequence source isolation is possible in parallel line applications [9] [10].

In summary, this paper offers guidance to select the proper polarization of the ground reactance element in quadrilateral distance protection. It outlines practical criteria for choosing the appropriate polarization method and validates the findings using field data and case studies, addressing the challenges posed by the changing dynamics of modern power systems.

## II. REVIEW OF REACTANCE ELEMENT BEHAVIOR IN THE IMPEDANCE PLANE

To illustrate how the polarizing quantity affects the reach of the reactance element, consider a fault at a distance  $m$  (pu) from the relay as shown in Fig. 3.

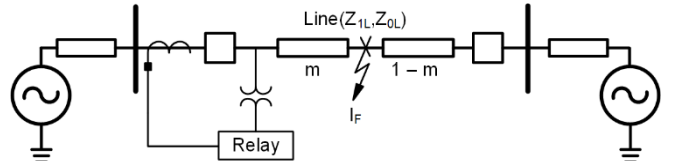


Fig. 3. Two-source power system with a single-line-to-ground fault at a distance  $m$  (pu) from the relay.

The voltage  $V_{\phi}$  at the relay location can be expressed as shown in (6).

$$V_{\phi} = m \cdot Z_{1L} \cdot I_{\phi\text{LOOP}} + I_F \cdot R_F \quad (6)$$

where  $I_F$  is the fault current and  $R_F$  is the fault resistance.

Dividing both sides of (6) by the polarizing current  $I_{POL}$  and taking imaginary parts results in (7).

$$\text{Im} \left[ \frac{V_\phi}{I_{POL}} \right] = \text{Im} \left[ \frac{m \cdot Z_{1L} \cdot I_{\phi LOOP}}{I_{POL}} \right] + \text{Im} \left[ \frac{I_F \cdot R_F}{I_{POL}} \right] \quad (7)$$

Writing  $\left( \text{Im} \left[ \frac{I_F \cdot R_F}{I_{POL}} \right] \right)$  from (7) in polar form results in (8).

$$\text{Im} \left[ \frac{V_\phi}{I_{POL}} \right] = \text{Im} \left[ \frac{m \cdot Z_{1L} \cdot I_{\phi LOOP}}{I_{POL}} \right] + \left| \frac{I_F \cdot R_F}{I_{POL}} \right| \sin(\angle I_F - \angle I_{POL}) \quad (8)$$

In (8), when the polarizing quantity angle ( $\angle I_{POL}$ ) equals the fault current angle ( $\angle I_F$ ), the term  $\sin(\angle I_F - \angle I_{POL})$  becomes zero. Consequently, the relay-calculated impedance, expressed as  $\left( \text{Im} \left[ \frac{V_\phi}{I_{POL}} \right] \right)$ , corresponds directly to the line reactance  $\left( \text{Im} \left[ \frac{m \cdot Z_{1L} \cdot I_{\phi LOOP}}{I_{POL}} \right] \right)$  from the relay terminal to the fault location. This alignment eliminates reach errors.

To illustrate the behavior of reactance elements in the apparent impedance plane, consider the A-phase-to-ground (AG) fault scenario shown in Fig. 4. For simplicity, the system is assumed to be perfectly homogeneous in the negative-sequence and zero-sequence networks. No tilt angle compensation is applied to the reactance elements. The fault is simulated at the relay reach point ( $m = 0.8$  pu) with a fault resistance of  $10 \Omega$  under outgoing and incoming load flow conditions.

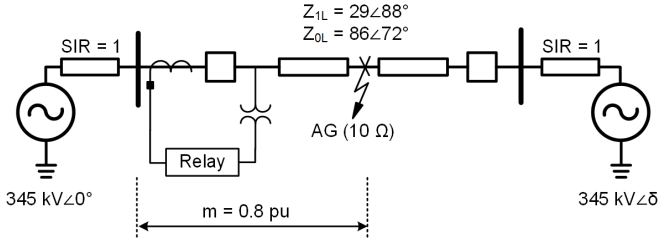


Fig. 4. AG fault at the reactance element reach ( $m = 0.8$  pu) with fault resistance of  $10 \Omega$  primary.

Table I shows that the loop current ( $I_{\phi LOOP}$ ) angle does not align with the fault current ( $I_F$ ) angle, whereas the sequence currents ( $I_0$  or  $I_2$ ) do. Here,  $I_2$  is the negative-sequence current.

TABLE I  
VOLTAGE AND CURRENTS FOR AG FAULT IN THE SYSTEM OF  
FIG. 4 UNDER OUTGOING AND INCOMING LOADS

Analogs	Outgoing Load ( $\delta = -15^\circ$ )	Incoming Load ( $\delta = 15^\circ$ )
$V_A$ (kV)	$110.4 \angle 55^\circ$	$122.2 \angle 63^\circ$
$I_{ALoop}$ (A)	$4,175 \angle 0^\circ$	$3,507 \angle 0^\circ$
$\angle I_F$ ( $^\circ$ )	$-6^\circ$	$27^\circ$
$\angle I_2$ ( $^\circ$ )	$-6^\circ$	$27^\circ$
$\angle I_0$ ( $^\circ$ )	$-6^\circ$	$27^\circ$

In this paper, a sequence network is considered homogeneous when the angle differences of the line and source impedances in that network do not exceed 10 degrees. If the angle difference exceeds 10 degrees, the network is considered nonhomogeneous.

In the apparent impedance plane for the outgoing load, shown in Fig. 5a, the negative-sequence or zero-sequence current-polarized reactance element drawn at the reach point accurately reflects the apparent impedance without reach error. In contrast, the loop current-polarized element, due to its leading angle relative to  $I_F$ , results in overreach. For the incoming load (Fig. 5b), the sequence-polarized element inherently tilts counterclockwise, following the fault current angle, while the static loop-polarized element underreaches. Note that the loop current-polarized reactance element line is static and parallel to the R-axis when there is no tilt compensation. In contrast, the negative-sequence and zero-sequence current-polarized reactance elements are oriented at angles of  $(\angle I_2 - \angle I_{\phi LOOP})$  and  $(\angle I_0 - \angle I_{\phi LOOP})$ , respectively, in the apparent impedance plane.

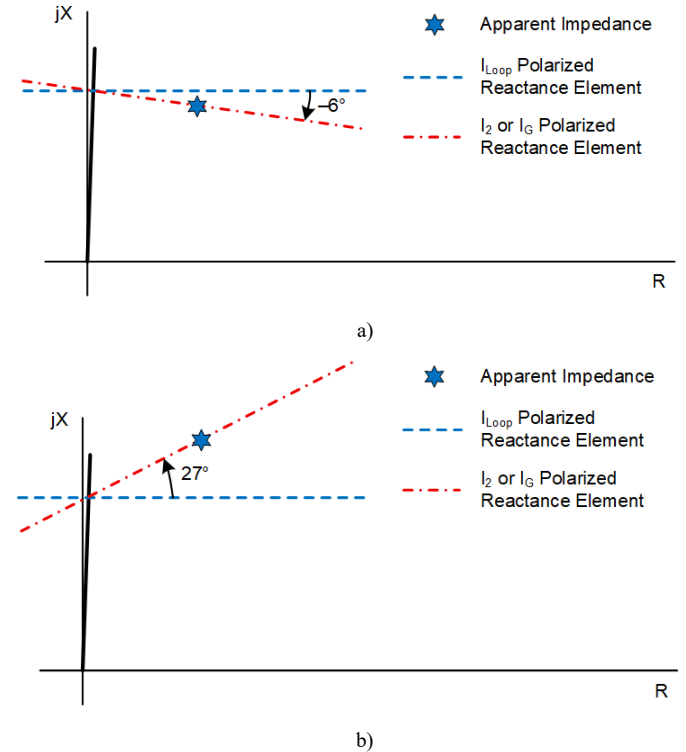


Fig. 5. Apparent impedance for the fault described in Fig. 4 for a) outgoing load and b) incoming load.

The inherent tilt in negative-sequence and zero-sequence currents to align with the fault current angle reduces reach errors, as (8) indicates. Depending on power flow direction, the element tilts clockwise or counterclockwise in the impedance plane. The example in Fig. 4 assumes a perfectly homogeneous system, where no tilt angle correction is needed. However, in nonhomogeneous systems, the tilt angle compensation must be applied to maintain security for underreaching zones (Zone 1).

Since the loop current-polarized reactance element is static in the impedance plane, it introduces overreach or underreach errors for resistive faults under moderate to heavy loading conditions. This element requires clockwise tilt compensation to ensure secure operation. A typical setting for underreaching zones is  $-15$  degrees [11]. However, in some cases, this default tilt angle may not be sufficient compensation and may need to be modified for heavy outgoing loading conditions.

### III. PERFORMANCE ANALYSIS OF DIFFERENT CURRENT-POLARIZED REACTANCE ELEMENTS

In the previous section, we established an understanding that the loop current-polarized reactance element remains static in the apparent impedance plane, while the negative-sequence- and zero-sequence-polarized elements exhibit dynamic tilt depending on power flow direction. We now proceed to evaluate the performance of these reactance elements from local and remote relay perspectives for faults occurring in the protected line section.

#### A. Sequential Tripping Under Resistive Fault Conditions

We analyze a 50-mile transmission line interconnecting two systems with power flow from the local terminal toward the remote terminal, as illustrated in Fig. 6. The AG fault with a fault resistance of  $15 \Omega$  primary is simulated at 0.5 pu distance from the local terminal. Consider Zone 1 and Zone 2 set to 0.8 pu and 1.2 pu of the line impedance in the relays at both terminals, respectively. The R by X ratio of the quadrilateral characteristic is set at 2, and no tilt is considered for the reactance elements. The system network is assumed to be perfectly homogeneous; therefore, the performance of negative-sequence- and zero-sequence-polarized reactance elements is identical.

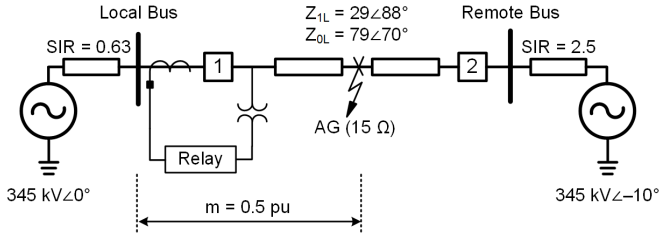


Fig. 6. 50-mile transmission line connecting two systems with an AG fault ( $R_F = 15 \Omega$  primary) at 0.5 pu from the local terminal.

Fig. 7 presents the quadrilateral distance characteristics for relays at the local and remote terminals. The reactance elements are polarized using the loop current.

From Fig. 7, it is evident that the relay at the local terminal, which measures outgoing power flow, detects the fault inside Zone 1 and can correctly initiate a Circuit Breaker 1 trip instantaneously. In contrast, the remote terminal relay, which measures incoming power, detects the fault in Zone 2 and, therefore, cannot initiate a Circuit Breaker 2 trip instantaneously.

Initially, it may seem that the remote relay must wait for the Zone 2 intentional delay to expire before issuing a trip command to Circuit Breaker 2. However, as shown in Fig. 8, once the local relay clears the fault by tripping Circuit Breaker 1, the remote relay detects the apparent impedance in Zone 1, allowing the remote relay to initiate a Circuit Breaker 2 trip and isolate the faulted phase.

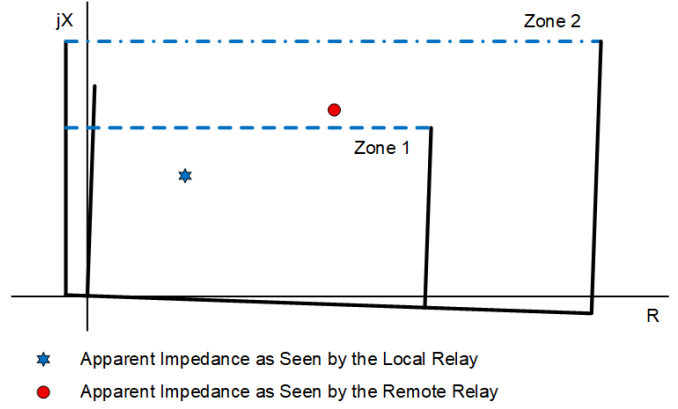


Fig. 7. Apparent impedances as observed by the local and remote relays with loop current-polarized reactance elements for the fault conditions described in Fig. 6.

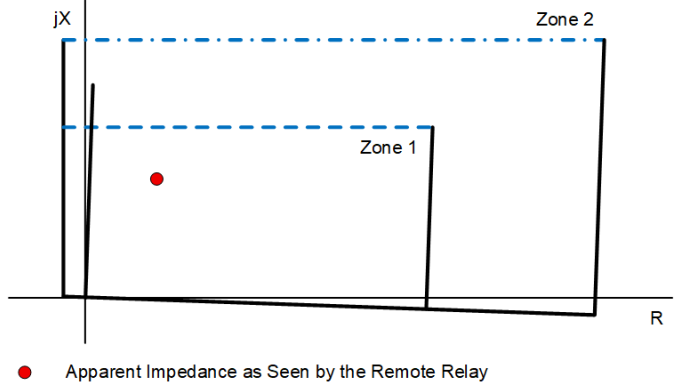


Fig. 8. Apparent impedance observed by the remote relay after fault clearance at the local terminal.

Fig. 7 and Fig. 8 show that in step distance applications, sequential tripping occurs in the presence of resistive faults under moderate to heavy loading conditions. The expected simultaneous Zone 1 pickup by local and remote relays does not occur with loop current polarization for this operating condition. When a communications-assisted protection scheme is used, the remote relay tripping is delayed by the communications time required to transmit the key signal from the local to the remote terminal.

Next, we analyze the performance of sequence current-polarized reactance elements. Fig. 9 shows the quadrilateral distance characteristics when the reactance elements are polarized using negative-sequence or zero-sequence current. In this case, the fault is detected well within Zone 1 by the local and remote relays, enabling instantaneous tripping at both ends, unlike the case with the loop current-polarized reactance element. This improved performance is due to the reactance element tilt introduced by sequence current polarization. As explained in Section II, sequence currents follow the fault current angle, unlike loop currents, improving the dependability of distance elements for resistive faults under moderate to heavy loading conditions.

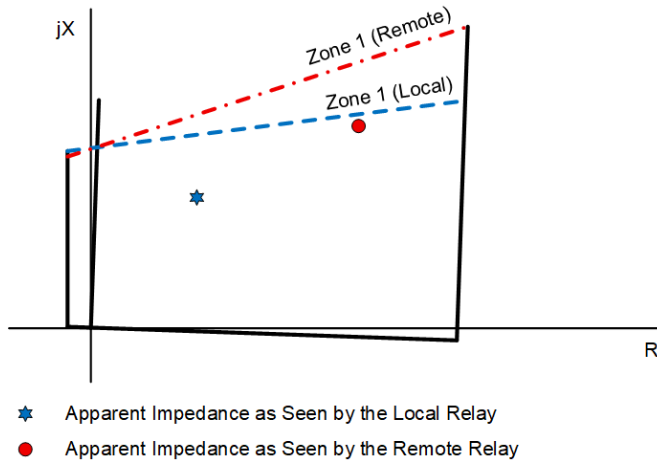


Fig. 9. Apparent impedances observed by the local and remote relays with a negative-sequence or zero-sequence current-polarized reactance element for the fault conditions described in Fig. 6.

### B. Delayed Tripping Under Resistive Fault Conditions

This section analyzes a resistive fault simulated near the Zone 1 reach. Fig. 10 shows an AG fault with a primary fault resistance of  $25 \Omega$  simulated at  $0.75$  pu distance from the local bus and power flow from the local to the remote bus. Consider Zone 1 and Zone 2 set to  $0.8$  pu and  $1.2$  pu of the line impedance in the relays at the terminals.

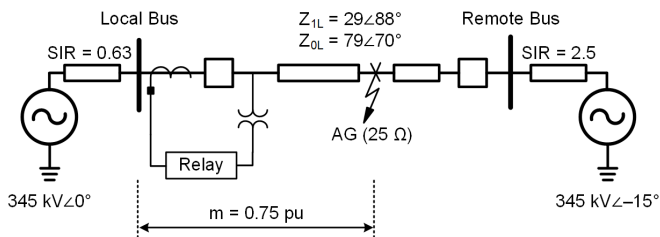


Fig. 10. 50-mile transmission line connecting two systems with an AG fault ( $R_F = 25 \Omega$  primary) at  $0.75$  pu from the local terminal.

With a loop-polarized reactance element, the relays at both terminals detect the fault within Zone 2 and outside Zone 1, as illustrated by the apparent impedances in Fig. 11.

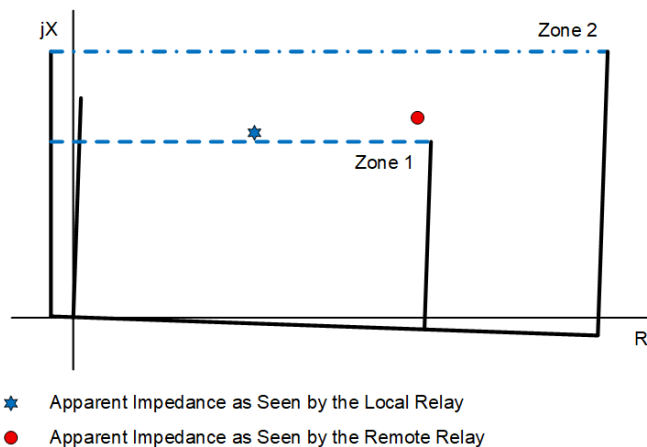


Fig. 11. Apparent impedances observed by the local and remote relays with a loop current-polarized reactance element for the fault conditions shown in Fig. 10.

Although the actual fault is within the Zone 1 reach of both relays, neither asserts to trip the circuit breakers instantaneously. Fault isolation can eventually occur through either a communications-assisted or step distance protection scheme. In the case of a communications-assisted scheme, fault isolation is delayed due to communications latency. For step distance schemes, the fault is cleared only after the Zone 2 timer expires, which generally ranges from 200 to 400 milliseconds.

Alternatively, when a sequence current-polarized reactance element is used, the local and remote relays accurately identify the fault within Zone 1, enabling the relay to trip instantaneously. This is shown in the apparent impedances shown in Fig. 12, which includes the Zone 1 distance characteristics of the local and remote relays using a negative-sequence- or zero-sequence-polarized reactance element. This desirable performance is due to the sequence-polarized reactance element dynamic tilt that follows the fault current angle.

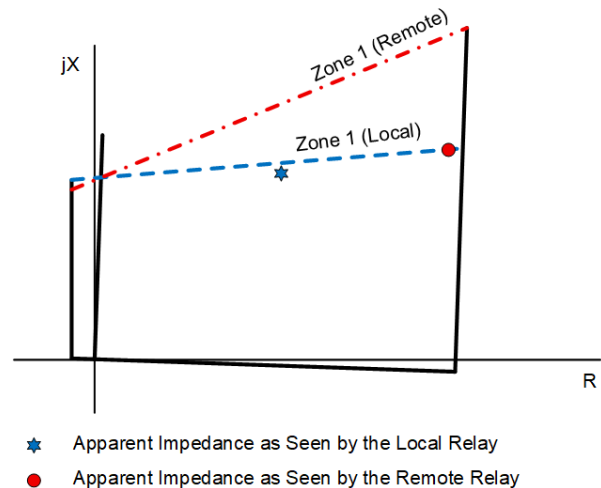


Fig. 12. Apparent impedances observed by the local and remote relays with a negative-sequence or zero-sequence current-polarized reactance element for the fault conditions described in Fig. 10.

### C. Fault Resistance Coverage

The fault resistance coverage is analyzed for a distance function, utilizing loop, negative-sequence, and zero-sequence current-polarized reactance elements for the system configuration illustrated in Fig. 13. The system network is assumed to be perfectly homogeneous; therefore, the performance of negative-sequence- and zero-sequence-polarized reactance elements is identical. The line relay under test is located at the local bus, and outgoing ( $\delta = -10^\circ$ ) and incoming ( $\delta = 10^\circ$ ) power flow conditions are considered.

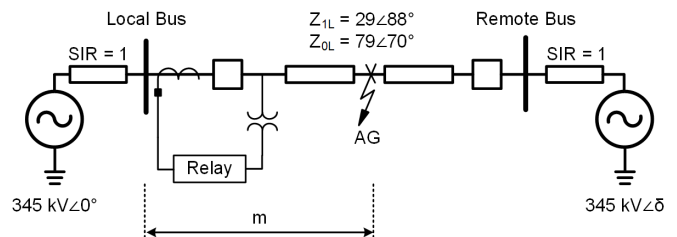


Fig. 13. 50-mile transmission line connecting two systems with an AG fault.

To evaluate the maximum fault resistance coverage along the line under outgoing and incoming loading conditions, the following characteristics of the distance function are considered:

- Left-side resistance blinder: Oriented parallel to the reactance axis in the apparent impedance plane; set at 10 percent of the positive-sequence line impedance.
- Right-side resistance blinder: Aligned parallel to the line impedance; set at four times the reach impedance in the impedance plane.
- Tilt angles: The loop current-polarized reactance element is tilted at  $-15$  degrees and the zero-sequence current-polarized element at  $-7$  degrees, as per the default settings in [11].

Fig. 14a and Fig. 14b illustrate that reactance elements with sequence polarization have better fault resistance coverage than elements with loop current polarization. As discussed in Sections II and III, the inherent ability of negative-sequence and zero-sequence currents to track the fault current angle helps to reduce reactance reach errors, even under high fault resistance conditions.

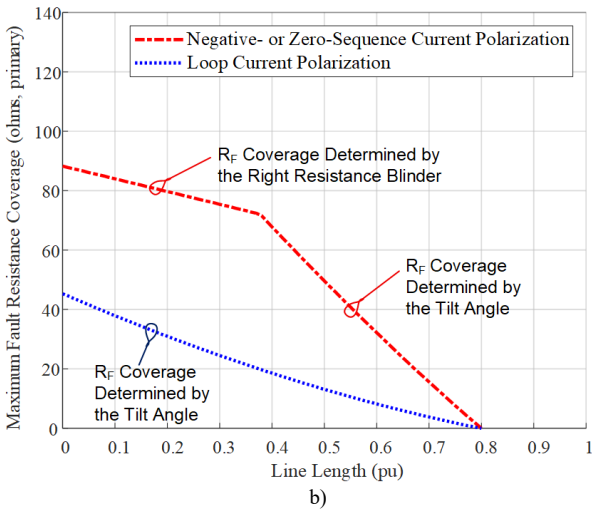
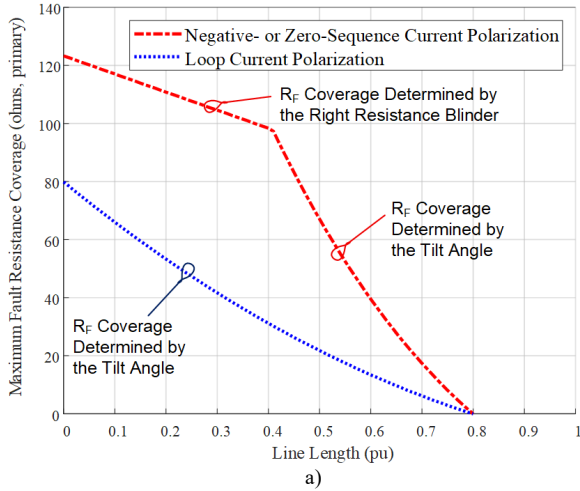


Fig. 14. Maximum fault resistance coverage using negative-sequence-, zero-sequence-, and loop current-polarized reactance elements for a) outgoing load ( $\delta = -10^\circ$ ) and b) incoming load ( $\delta = 10^\circ$ ).

Fig. 14a and Fig. 14b show that the maximum fault resistance coverage for the quadrilateral distance function with a sequence current-polarized reactance element is initially determined by the right resistance blinder. However, as the distance to the fault increases, the tilt angle of the reactance element becomes the determining factor. In contrast, the maximum fault resistance coverage for the quadrilateral distance function with a loop current-polarized reactance element is determined solely by the tilt angle of the reactance element.

Another key observation is that fault resistance coverage is higher under outgoing load conditions than when the relay is measuring incoming load. Also, the improved fault resistance coverage provided by sequence current-polarized reactance elements enhances the likelihood of instantaneously detecting resistive faults within Zone 1, thereby reducing the chances of sequential or delayed tripping, as previously discussed.

#### IV. IMPACT OF PARALLEL LINE MUTUAL COUPLING ON THE ANGLE OF POLARIZING QUANTITIES

Fig. 15 illustrates typical configurations of parallel transmission lines. Even when the lines differ in length, their arrangements can generally be categorized into one of the configurations shown in this figure.

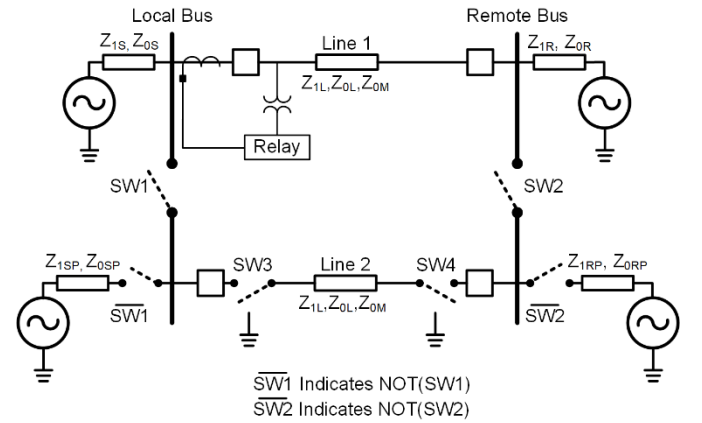


Fig. 15. Network representing various parallel line configurations.

Switch SW1 indicates whether the parallel lines share a common bus at the local terminal. Switch SW2 indicates whether the parallel lines share a common bus at the remote terminal. If either SW1 or SW2 is open, the corresponding terminal, local or remote, will have a separate source for each line. Switches SW3 and SW4 reflect the operational status of the parallel line, that is, whether the line is in or out of service. When the parallel line is out of service, it is assumed to be grounded at both ends or at one end.

In Fig. 15:

$Z_{1S}$  is the positive-sequence local-source impedance of the faulted line.

$Z_{1R}$  is the positive-sequence remote-source impedance of the faulted line.

$Z_{1SP}$  is the positive-sequence local-source impedance of the parallel line.

$Z_{1RP}$  is the positive-sequence remote-source impedance of the parallel line.

- $Z_{0S}$  is the zero-sequence local-source impedance of the faulted line.
- $Z_{0R}$  is the zero-sequence remote-source impedance of the faulted line.
- $Z_{0SP}$  is the zero-sequence local-source impedance of the parallel line.
- $Z_{0RP}$  is the zero-sequence remote-source impedance of the parallel line.
- $Z_{0M}$  is the zero-sequence mutual coupling impedance.

#### A. Calculating the Tilt Angle (Load Correction Angle) for Loop Current Polarization

The loop current for different fault types is a function of a corresponding phase current. In the case of resistive faults, the loop currents include fault and load components, making it difficult to determine the fault current angle.

A correction angle, referred to as a tilt angle, is required to ensure security of the underreaching loop current-polarized reactance element. This angle represents the difference between the fault current angle at the fault location and the measured loop current angle for maximum outgoing loading conditions. The tilt angle is determined as the minimum angle (e.g.,  $-15$  degrees) obtained from a series of faults simulated with different fault resistances at the remote end of the protected line [12]. Equation (9) provides the expression for this tilt angle. Note that for different parallel line configurations, a modified zero-sequence compensation factor may be necessary to ensure that the Zone 1 element underreaches and the Zone 2 element overreaches [7] [8].

$$T_1 = \min \left[ \arg \left( \frac{I_F}{I_{\phi LOOP}} \right) \forall 1 \leq R_F \leq 100 \right] \quad (9)$$

#### B. Calculating the Tilt Angle (Nonhomogeneous Network Correction Angle) for Negative-Sequence Current Polarization

The negative-sequence current polarization tilt angle, where the parallel lines originate and terminate on common buses (i.e., SW1 and SW2 closed in Fig. 15), is given by (10) [12].

$$T_{12} = -\arg \left[ \frac{(1-m) \cdot (Z_{2S} + Z_{1L} + Z_{2R}) + Z_{2R}}{2 \cdot (Z_{2S} + \frac{Z_{1L}}{2} + Z_{2R})} \right] \quad (10)$$

where  $Z_{2S}$  and  $Z_{2R}$  are negative-sequence local- and remote-source impedances, respectively.

For other configurations, when the lines originate from different buses but terminate at a common bus or when the lines originate and terminate on separate buses, the negative-sequence mutual coupling between the parallel lines is negligible and can be ignored [7]. In such cases, the tilt angle should be calculated by treating the system as a single-line configuration, using (11) [11] [12]. Note that in these cases, the Thevenin equivalent impedance may include the parallel line impedance. Also, note that the lowest tilt angle evaluated for faults at the reach and end of the line needs to be used.

$$T_{12\_SL} = \arg \left[ \frac{Z_{2S\_Thevenin} + Z_{2L} + Z_{2R\_Thevenin}}{(1-m) \cdot Z_{2L} + Z_{2R\_Thevenin}} \right] \quad (11)$$

where  $Z_{2S\_Thevenin}$  and  $Z_{2R\_Thevenin}$  are negative-sequence local- and remote-source Thevenin equivalent impedances, respectively.

As is evident from (10) and (11), the tilt angle required to align the negative-sequence current with the fault current angle depends only on the negative-sequence system parameters. This sole dependence has made negative-sequence current a default and widely used choice for polarizing the reactance element. However, with the increasing integration of IBRs, the negative-sequence current contribution from the IBR becomes unreliable under fault conditions [13] [14]. Therefore, the increase in IBR penetration compromises the reliability of the power system protection when using negative-sequence current for polarization of the reactance element [6].

#### C. Calculating the Tilt Angle (Nonhomogeneous Network Correction Angle) for Zero-Sequence Current Polarization

For a single-line configuration, the tilt angle for zero-sequence current polarization follows (11), using the zero-sequence network impedances instead of negative-sequence parameters [11]. In contrast, for parallel line configurations, the presence of zero-sequence coupling between the parallel lines implies that the expression used for the negative-sequence network, (10), is not applicable for zero-sequence current polarization. As the appendix describes, the zero-sequence current polarization tilt angle in such configurations depends on the zero-sequence parameters, including source, line, and mutual coupling impedances, as well as fault location.

The appendix has the expressions for zero-sequence current tilt angle compensation for each possible parallel line configuration in the network of Fig. 15. These expressions indicate that the tilt angle is unaffected by the zero-sequence current in the parallel line. Instead, it is determined by the zero-sequence network parameters and fault location, as indicated in (12).

$$T_{1G} = f(Z_{0S}, Z_{0SP}, Z_{0L}, Z_{0M}, Z_{0R}, Z_{0RP}, m) \quad (12)$$

#### D. Analyzing the Performance of Negative- and Zero-Sequence Current-Polarized Reactance Elements in a Parallel Line Configuration

To demonstrate that the negative-sequence and zero-sequence current-polarized reactance elements behave similarly in parallel line configurations, consider a homogeneous parallel line system, as illustrated in Fig. 16 and Fig. 17. In Fig. 16, both lines originate and terminate at a common bus, whereas in Fig. 17, they originate from a common bus but terminate at separate buses. The systems are considered perfectly homogeneous, except for the zero-sequence mutual coupling impedance angle, which in this case is 60 degrees.

In the negative-sequence network, as per (10) or (11), the network homogeneity ensures a tilt angle of 0 degrees for faults anywhere along the length of the line. However, in the zero-sequence network, due to the mutual coupling impedance angle of 60 degrees, the network becomes nonhomogeneous, requiring tilt angle compensation. The expressions from the appendix can be used to calculate the tilt angle at each point along the line depending on the parallel line configuration.

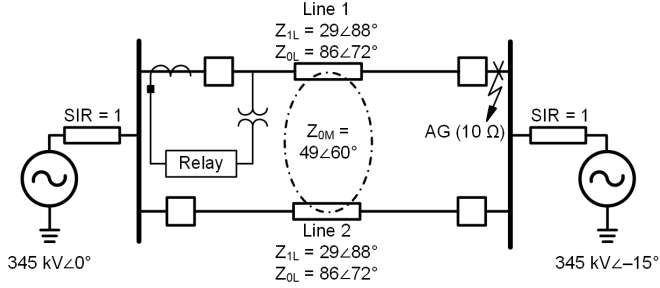


Fig. 16. Network with parallel lines that originate and terminate at a common bus with an AG fault at the remote bus.

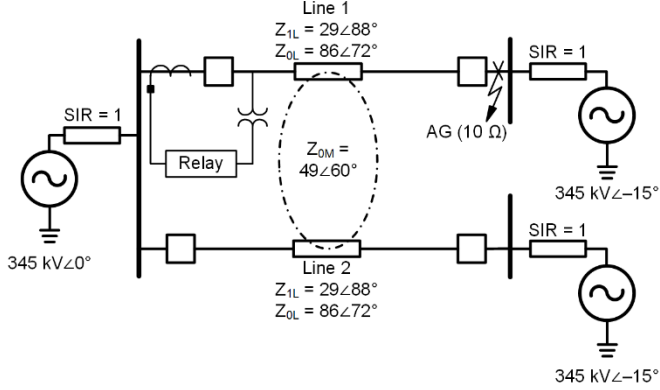


Fig. 17. Network with parallel lines that originate at a common bus and terminate at separate buses with an AG fault at the remote bus of the protected line (Line 1).

Fig. 18 presents the zero-sequence current tilt angle for common and split bus configurations (Fig. 16 and Fig. 17). Since the simulated AG fault is at the remote bus, the tilt angle at that location is considered for the reactance element calculations.

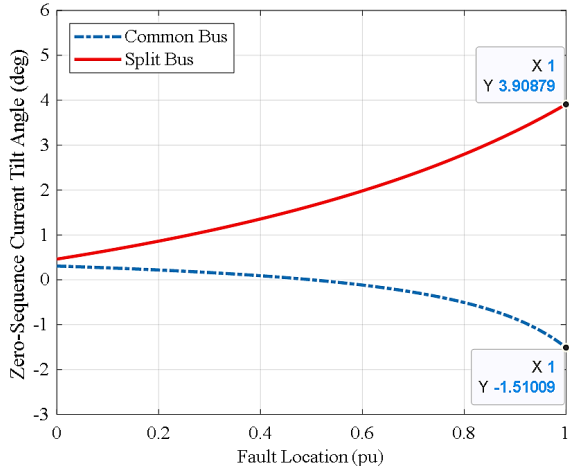


Fig. 18. Zero-sequence current polarization tilt angle along the length of the line for common and split bus parallel line configurations.

Table II summarizes the voltage and current phasors for a fault at the remote bus, as illustrated in Fig. 16 and Fig. 17. It can be observed that the relay-measured negative-sequence current angle aligns with the actual fault current angle. In contrast, as Table II shows, the zero-sequence current angle does not align with the fault current angle, but once the calculated tilt is applied, it does. After applying the tilt compensation, the reactance calculated from (3) using

zero-sequence current polarization matches exactly with that obtained using negative-sequence current polarization. This confirms that the performance of zero-sequence current-polarized reactance elements can be equivalent to that of negative-sequence current-polarized elements even in parallel line configurations.

TABLE II  
VOLTAGE AND CURRENTS FOR AG FAULT IN  
THE SYSTEM OF FIG. 16 AND FIG. 17

Analogs	Common Bus (Fig. 16)	Split Remote Bus (Fig. 17)
$V_{\phi}$ (kV)	113.4 $\angle$ 0°	141 $\angle$ 0°
$I_{\phi, LOOP}$ (A)	2,252 $\angle$ -42.7°	4,869 $\angle$ -62.3°
$\angle I_F$ (°)	-45.3°	-55.9°
$\angle I_2$ (°)	-45.3°	-55.9°
$T_{12}$ (°)	0°	0°
$X_{AG, I2}$ (pu)	1.23	0.83
$\angle I_0$ (°)	-43.8°	-59.8°
$T_{10}$ (°)	-1.5°	3.9°
$X_{AG, I0}$ (pu)	1.23	0.83

It is important to note that this analysis is intended to show the equivalence in behavior between the negative-sequence and zero-sequence polarization methods in parallel line configurations. However, irrespective of the polarizing quantity choice, the impact of the zero-sequence mutual voltage drop along the faulted line will cause the reactance calculation to underreach or overreach. From Table II, for the common bus configuration simulation, an underreach effect is observed, while in the split remote bus configuration simulation, the relay exhibits overreach. These reach errors in parallel line configurations can be mitigated through use of an appropriate zero-sequence compensation factor or by adjusting the relay reach settings [7] [8].

## V. CRITERIA FOR CHOOSING THE GROUND REACTANCE ELEMENT POLARIZING QUANTITY

Fig. 19 illustrates the flowchart that outlines the criteria for selecting the reactance element polarizing quantity for the quadrilateral ground distance element.

Referring to the flowchart, the outlined criteria need to be followed to determine the appropriate polarizing quantity for the ground reactance element:

1. The strength of the negative-sequence source impedances at the local and remote terminals needs to be evaluated under worst-case contingencies. A weak source is typically indicated by IBRs or radial loads behind the relay terminal. Conversely, conventional sources (synchronous generators) suggest a strong source. If any of the sources are weak, the zero-sequence source network needs to be evaluated. See Number 3.

2. If the sources at the local and remote terminals are strong, under worst-case contingencies, the negative-sequence network homogeneity needs to be evaluated.
  - a) Homogeneous negative-sequence network: A negative-sequence network is typically homogeneous when conventional sources are present at local and remote terminals, and the positive-sequence line impedance angle closely matches the source impedance angle (e.g., the impedance angle difference does not exceed 10 degrees). An overhead transmission line connecting two grid systems with conventional sources typically has a homogeneous negative-sequence network. In such cases, the default tilt angle setting for the ground reactance element ( $TANGG = -7^\circ$ ) is generally adequate. However, it is advisable to calculate the tilt angle as per the line configuration (e.g., single or parallel lines) using (10) or (11). The lowest tilt angle evaluated for faults at the reach and end of the line needs to be used. Applying the calculated tilt angle helps balance dependability and security.
  - b) Nonhomogeneous negative-sequence network: Nonhomogeneity typically occurs when the protected line is an underground cable or when there is a significant difference between the source and line impedance angles in the negative-sequence network (e.g., the impedance angle difference exceeds 10 degrees). In such cases, calculating the appropriate tilt angle is strongly recommended, as the default setting ( $TANGG = -7^\circ$ ) may not suffice. The minimum tilt angle evaluated for faults at the reach and end of the line must be used. If the local-source impedance is known but the remote-source impedance is uncertain, (13) must be used to determine the tilt angle, which is intentionally biased toward security, as described in Section IV of [12]. The 88 degree angle applied in (13) represents the highest negative-sequence source impedance angle under practical considerations.

$$T_{12} = \arg(Z_{2S} + Z_{2R}) - 88^\circ \quad (13)$$

If the local-source impedance is unknown or determining the tilt angle is not possible, the suitability of zero-sequence current for polarization needs to be considered. See Number 3.

3. The strength of the zero-sequence source impedances at the local and remote terminals under worst-case contingencies needs to be evaluated. A strong zero-sequence source is indicated through a grounded transformer neutral and a delta configuration in either secondary or tertiary windings. Radial loads without any transformer grounding source suggest a weak source. If the zero-sequence source is weak, evaluation of the zero-sequence network is not needed and a self-polarized reactance element ( $ESPQUAD = Y$ ) with an appropriate tilt angle, as per (9), needs to be considered.

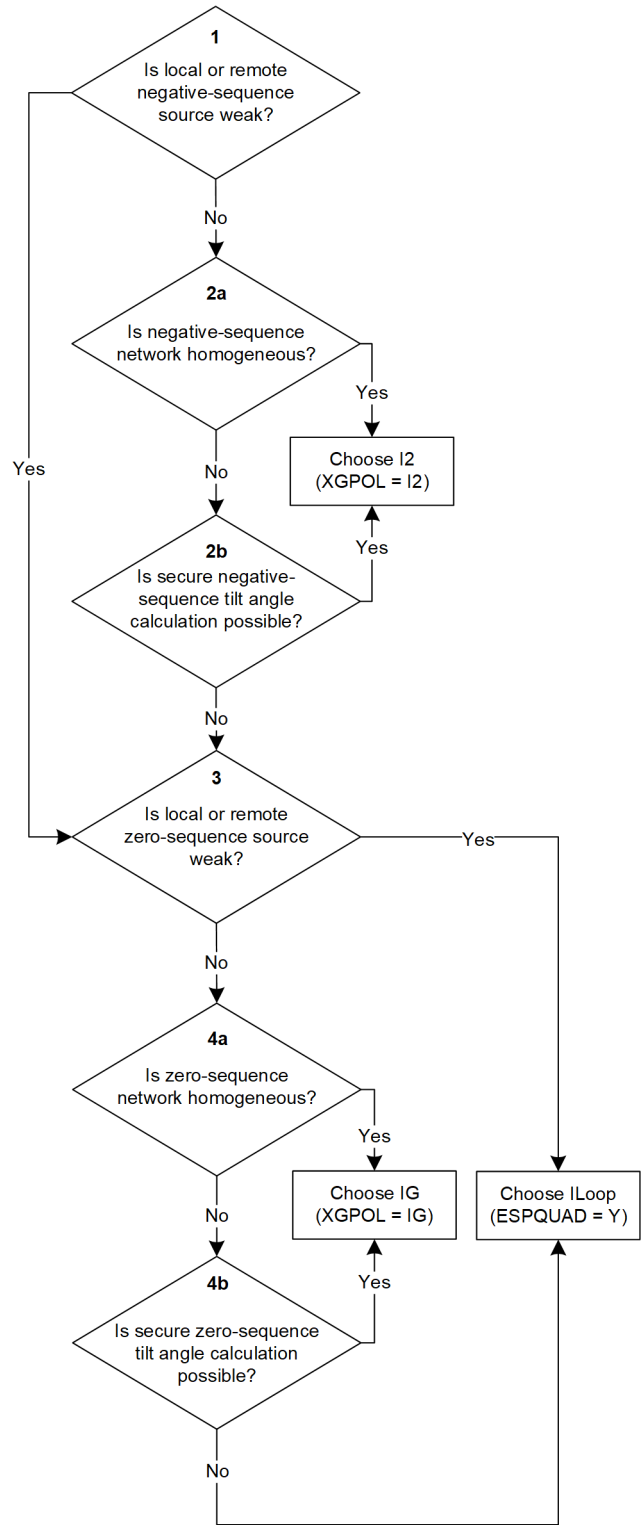


Fig. 19. Selection criteria for the ground reactance element polarizing quantity.

4. If the zero-sequence sources at the local and remote terminals are strong, under worst-case contingencies, the zero-sequence network homogeneity needs to be evaluated.
  - a) Homogeneous zero-sequence network: This condition is met when the angles of the local and remote sources and the zero-sequence line impedance are similar (e.g., the impedance angle difference does not exceed 10 degrees). In such cases, the default tilt angle ( $TANGG = -7^\circ$ ) is typically sufficient. However, it is recommended to calculate the tilt angle using (11) with zero-sequence parameters for a single-line configuration. For parallel line configurations, the equations derived in the appendix must be used. The minimum tilt angle evaluated for faults at the reach and end of the line across all configurations, which is described in the appendix, needs to be used. The implementation of such a tilt angle ensures a good balance between dependability and security.
  - b) Nonhomogeneous zero-sequence network: Nonhomogeneity typically occurs with underground cables or when there is a significant difference between the zero-sequence source and line impedance angles (e.g., the impedance angle difference exceeds 10 degrees). In such cases, calculating the appropriate tilt angle is strongly recommended, as the default setting ( $TANGG = -7^\circ$ ) will not be sufficient. The minimum tilt angle evaluated for faults at the reach and end of the line across all configurations, which is described in the appendix, must be used. If the local-source impedance is known but the remote-source impedance is uncertain, (14) must be used to determine the tilt angle, which is intentionally biased toward security, as described in Section IV of [12]. The 88 degree angle applied in (14) represents the highest zero-sequence source impedance angle under practical considerations.

$$T_{IG} = \arg(Z_{0S} + Z_{0R}) - 88^\circ \quad (14)$$

If calculating the tilt angle is not possible, a self-polarized reactance element ( $ESPQUAD = Y$ ) with an appropriate tilt angle, as per (9), needs to be considered.

## VI. FIELD EVENT ANALYSIS

Now that the criteria for selecting the appropriate polarizing quantity for the reactance element has been established, let us examine a couple of field events.

In this analysis, only the local-source impedance and line impedance values were available to the authors. Consequently, the correction angles were computed using an assumption for the remote-source impedance, intentionally biased toward security, as described in Section IV of [12]. Based on these inputs, the nonhomogeneity correction angle was calculated using (13) and (14) for each sequence network in the two field event cases that we analyzed. For the loop current-polarized

reactance element, a tilt angle of  $-15$  degrees (default value in [11]) was considered.

### A. Field Case 1

Fig. 20 illustrates the one-line diagram of a system in which an external CG fault occurred. The relay located at the local bus incorrectly issued a Zone 1 trip for this fault. An autotransformer with a delta tertiary winding was located behind the local relay, resulting in a current profile influenced by the zero-sequence component during the fault. The relay was programmed with negative-sequence current as the polarizing quantity for the reactance element, and the nonhomogeneity correction tilt angle was set at  $-3$  degrees.

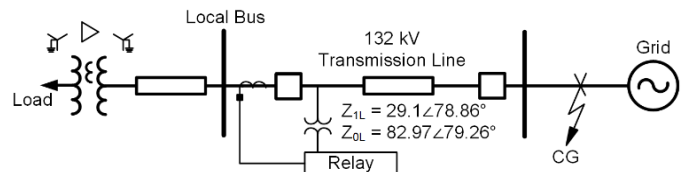


Fig. 20. 87.9 km transmission line with an external CG fault beyond the remote terminal.

Fig. 21 presents the sequence current magnitudes recorded during the fault event. The data show that the zero-sequence current magnitude ( $3I0\_MAG\_SEC$ ) is more stable than the negative-sequence current magnitude ( $3I2\_MAG\_SEC$ ).

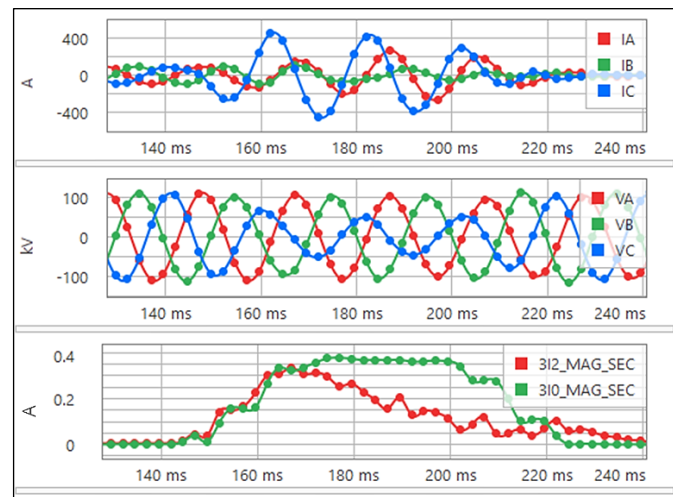


Fig. 21. Negative-sequence and zero-sequence current magnitudes during the external CG fault.

In Fig. 22,  $Z2S\_MAG\_SEC$  and  $Z2S\_ANG$  represent the negative-sequence source impedance magnitude and angle, respectively, behind the relay, and  $Z0S\_MAG\_SEC$  and  $Z0S\_ANG$  indicate the zero-sequence source impedance magnitude and angle, respectively, behind the relay. For a forward fault, these sequence source impedances are calculated as the negative ratio of the respective sequence voltage to the sequence current. During a fault, the negative-sequence source impedance is notably weak, primarily due to the presence of only load impedance behind the relay terminal. If the rest of the power system exhibits impedance angles between 80 and 90 degrees, the angle of the negative-sequence source impedance ( $Z2S\_ANG$ ) is low and unstable, as shown in

Fig. 22. The negative-sequence source calculations indicate a highly nonhomogeneous and unreliable network. Therefore, negative-sequence current is not a suitable polarizing quantity for this system.

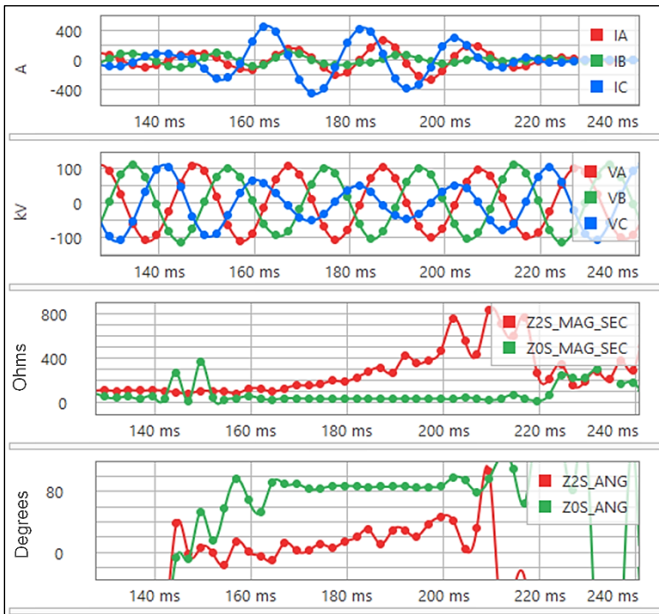


Fig. 22. Negative-sequence and zero-sequence source impedances during the external CG fault.

Applying the same analysis to the zero-sequence network reveals that, during the fault, the zero-sequence source impedance remains more stable than the negative-sequence source impedance, with an angle close to 88 degrees. This pattern indicates a more homogeneous network, consistent with the line angle (79 degrees) and remote-source impedance angle.

Fig. 23 depicts the reactance calculation results for negative-sequence, zero-sequence, and loop current polarizations. Note that the results with negative-sequence polarization are constantly changing and crossing the reach line, causing the misoperation, indicated by XCG1F, whereas the zero-sequence- and loop-polarized calculations, represented by X\_CALC\_I0 and X\_CALC\_LOOP, respectively, are much more stable than the negative-sequence calculations, represented by X\_CALC\_I2, and never fall below the reach line.

In this scenario, the strength of the zero-sequence source and the homogeneity of the associated network make zero-sequence current a more suitable and dependable choice for polarization. While loop current polarization also offers stability and security, the reduced effectiveness in detecting resistive faults under moderate to heavy loading conditions limits its reliability. In this case, zero-sequence current stands out as the most appropriate and robust polarizing quantity compared to negative-sequence and loop current polarization, which is determined based on Fig. 19.

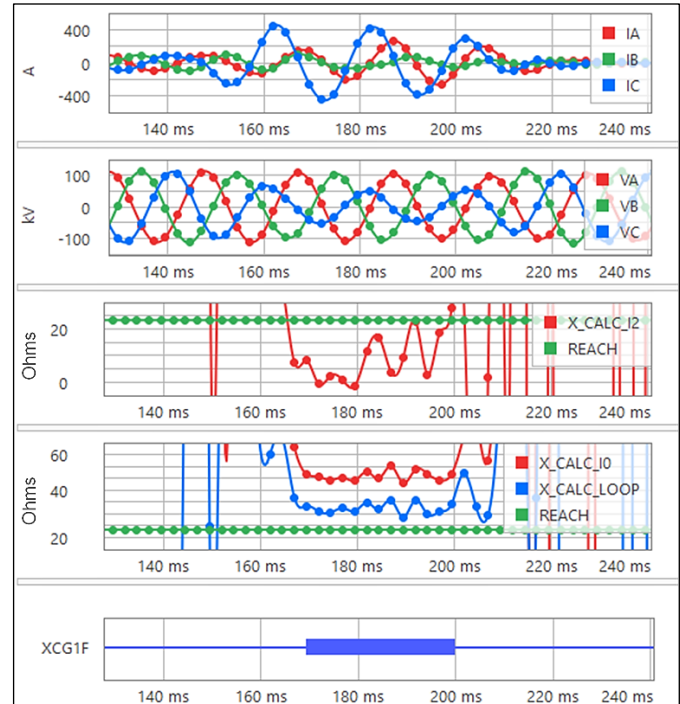


Fig. 23. Reactance calculations with negative-sequence, zero-sequence, and loop current polarizations.

## B. Field Case 2

Fig. 24 presents a simplified diagram of a system in which an external BG fault occurred on a parallel transmission line.

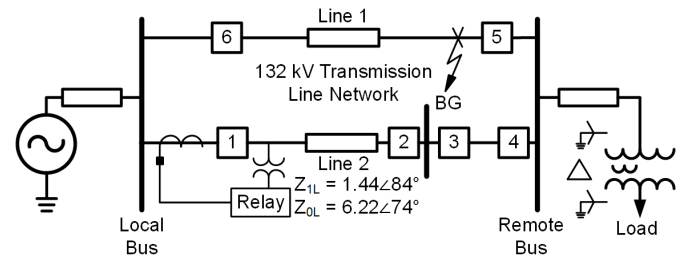


Fig. 24. 10.3 km transmission line (Line 2) connecting two systems with a BG fault on the parallel line (Line 1).

The relay protecting Line 2 at the local terminal incorrectly issued a Zone 1 trip. The relay was configured to use zero-sequence current as the polarizing quantity of the reactance element.

As shown in Fig. 25, the sequence current analysis reveals that during the initial fault in the forward direction, the negative-sequence current magnitude, indicated by 3I2\_MAG\_SEC, is the predominant component. However, when Circuit Breaker 5 opens, the current reverses and the relay measures pure zero-sequence current, indicated by 3I0\_MAG\_SEC, because the main source of current that the relay measures comes from a grounded transformer behind the remote bus, which is a strong zero-sequence current source.

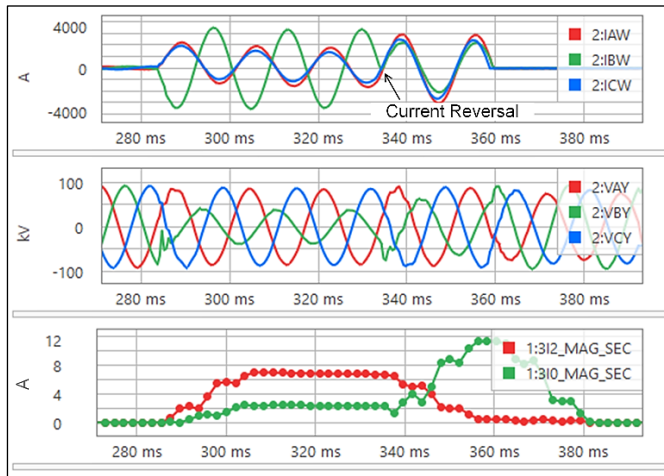


Fig. 25. Unfiltered phase currents and voltages and filtered negative-sequence and zero-sequence current magnitudes during the BG fault on the parallel line (Line 1).

In Fig. 26,  $Z2S\_MAG\_SEC$  and  $Z2S\_ANG$  represent the negative-sequence source impedance magnitude and angle, respectively, behind the relay, and  $Z0S\_MAG\_SEC$  and  $Z0S\_ANG$  indicate the zero-sequence source impedance magnitude and angle, respectively, behind the relay.

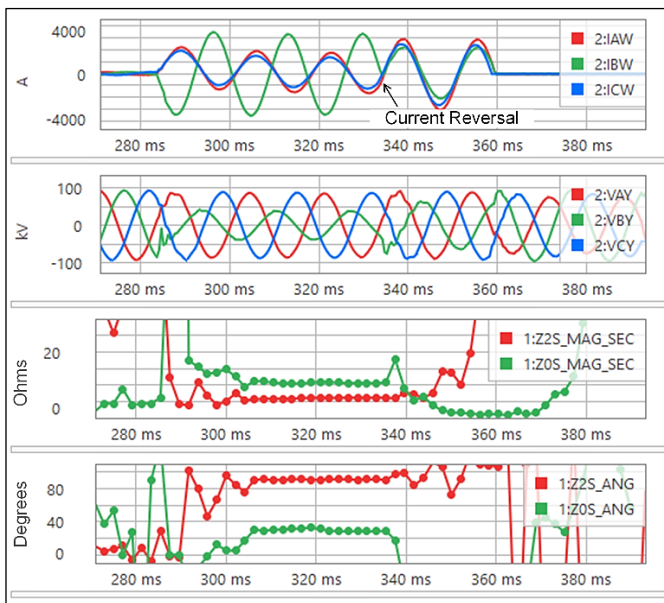


Fig. 26. Unfiltered phase currents and voltages and filtered negative-sequence and zero-sequence source impedances during the BG fault on the parallel line (Line 1).

The angle of the negative-sequence source impedance ( $Z2S\_ANG$ ) closely matches that of the line impedance (84 degrees), suggesting that the negative-sequence network may be relatively homogeneous. However, due to the presence of loads and the absence of a source beyond the remote bus, the magnitude and angle of the remote-source impedance become unreliable after the current reversal (when Circuit Breaker 5 opens). These operating conditions can result in an unreliable and highly nonhomogeneous network. As a result, while negative-sequence polarization may be effective for forward faults, it remains an unreliable polarizing quantity for faults behind the relay or on the parallel line when Circuit Breaker 5

is open. Now that it is determined that the negative-sequence current is not a suitable choice for polarization, let us evaluate the zero-sequence current as a polarizing quantity.

The zero-sequence source impedance angle ( $Z0S\_ANG$ ) behind the relay during the fault is observed to be between 30 and 40 degrees. In comparison, the zero-sequence line impedance angle is approximately 74 degrees, and the remote terminal includes a grounded source typically exhibiting an impedance angle between 80 and 90 degrees. This configuration indicates that the zero-sequence network is nonhomogeneous, though not weak at either the local or remote terminals.

Because both terminals have moderate to strong zero-sequence sources, zero-sequence current remains a viable polarizing quantity. However, due to the nonhomogeneity of the network, it is necessary to calculate and apply a tilt angle. Using (14), the required correction angle for the zero-sequence network is  $-40$  degrees. With this tilt applied, the reactance element using zero-sequence current polarization would operate securely. That said, the magnitude of the required tilt angle is significant, and determining it requires detailed analysis.

Fig. 27 illustrates the reactance calculation at the time of the misoperation.

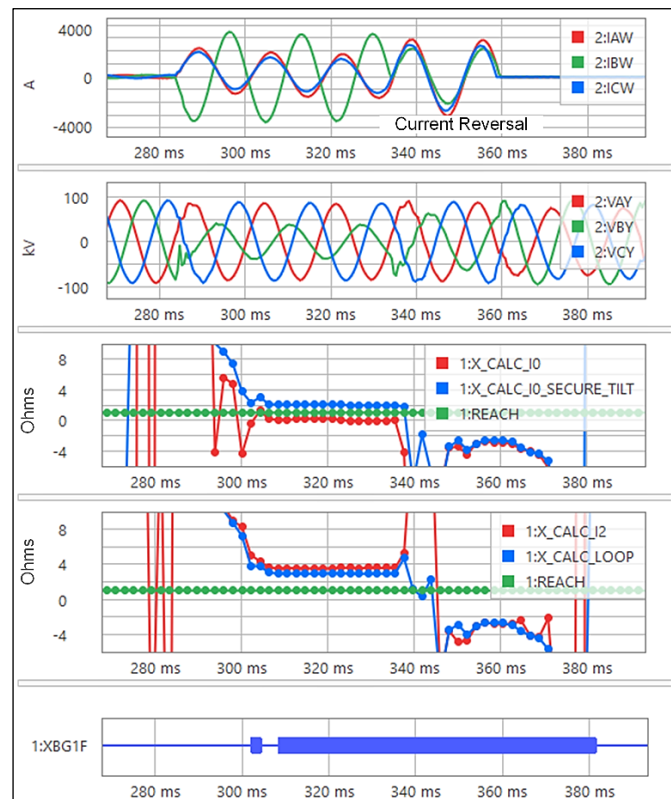


Fig. 27. Unfiltered phase currents and voltages and filtered reactance calculation with zero-sequence, negative-sequence, and loop polarizations.

The relay was configured to use zero-sequence current as the polarizing quantity with a correction angle of  $-7$  degrees, which led to an incorrect trip, indicated by XBG1F. Had the relay been programmed with the correct tilt angle of  $-40$  degrees, the  $X\_CALC\_I0\_SECURE\_TILT$  calculations show the

zero-sequence current-polarized reactance element would have operated securely.

In Fig. 27,  $X\_CALC\_I2$  represents the negative-sequence current-polarized reactance calculation (with a tilt angle of  $-2$  degrees) and  $X\_CALC\_LOOP$  represents the loop current-polarized calculation (with a default tilt angle of  $-15$  degrees). In the case of negative-sequence current polarization, the reactance never crosses the reach point, and the relay would have correctly restrained. However, as previously discussed, negative-sequence current polarization is not reliable for reverse faults or faults on the parallel line when current reversal occurs.

These results highlight the importance of understanding the source strength at both ends of the line. While negative-sequence polarization may appear suitable for forward faults, it becomes unreliable for reverse or parallel line faults because of the weak remote source. In such cases, zero-sequence polarization can be used, but only with a significant tilt angle, which requires detailed analysis. Therefore, the recommended approach is to use loop current polarization with a suitable tilt angle, as expressed in (9), which offers more reliable polarization than the other options, based on Fig. 19. Note in Fig. 27, following the current reversal, all the reactance calculations are below the reach setting. However, this is not a concern, as the directional element that supervises the quadrilateral distance protection interprets the current reversal as a reverse fault.

## VII. CONCLUSION

This paper presents a detailed investigation into the selection of polarizing quantities for reactance elements that are part of quadrilateral ground distance protection, addressing traditional practices and the challenges posed by modern power systems. While negative-sequence current has historically been favored because of the homogeneous nature of negative-sequence networks and the minimal impact from mutual coupling in parallel line applications, the increasing integration of IBRs and application of distance elements with weak sources have introduced significant variability in negative-sequence current sources. This evolution of the power system requires revisiting polarization practices of ground distance protection, particularly in systems where negative-sequence sources may be weak or unreliable.

This paper shows that using zero-sequence current polarization is a robust and dependable alternative for the ground reactance element even in parallel line applications with heavy mutual coupling. Analytical derivations confirm that the tilt angle required for zero-sequence polarization depends on the zero-sequence network parameters and is unaffected by currents in adjacent lines. Furthermore, the study clarifies that underreaching or overreaching errors are primarily caused by mutually coupled zero-sequence voltage along the line, rather than the choice of polarizing current. These errors can be

effectively mitigated through appropriate zero-sequence compensation factors or by adjusting the relay reach settings. Additionally, the performance of the ground directional elements that are part of the quadrilateral distance element characteristic needs to be evaluated in parallel line applications in case there is a possibility of zero-sequence source isolation.

The paper also compares the performance of loop current polarization with that of sequence current polarization under high fault resistance conditions and moderate to heavy loading conditions. It is demonstrated that loop-polarized reactance elements, due to their static characteristic, may result in sequential or delayed tripping, particularly in step distance protection schemes. In contrast, sequence-polarized reactance elements, whether negative- or zero-sequence, dynamically align with the fault current angle, enabling accurate Zone 1 detection and instantaneous tripping at both terminals, even in parallel line scenarios.

To support practical implementations, the paper introduces a structured decision-making framework for selecting the appropriate polarizing quantity. The proposed flowchart-based approach considers the presence of weak sources in negative- or zero-sequence networks, the homogeneity of the network, and the feasibility of a secure tilt angle calculation. When the negative-sequence network is strong and exhibits homogeneous behavior or when the tilt angle can be reliably calculated, negative-sequence current is the recommended polarizing quantity. Otherwise, if the zero-sequence network is robust and meets these criteria, zero-sequence current becomes the preferred choice. In scenarios where both sequence networks are characterized by weak terminals or significant nonhomogeneity that complicate tilt angle calculations, loop current polarization is identified as another possible alternative.

Finally, this study confirms that zero-sequence polarization performs equivalently to negative-sequence polarization in parallel line applications. The paper provides a validated criteria-driven methodology for selecting the most suitable polarizing quantity for the reactance element for quadrilateral ground distance protection. These findings and recommendations are supported by analytical derivations, simulation results, and real-world case studies, and they offer guidance for protection engineers to address challenges of the modern power system.

## VIII. APPENDIX

This appendix derives the angular relationship between the relay-measured zero-sequence current and the actual zero-sequence fault current for typical parallel line configurations. Fig. 28 illustrates the zero-sequence network for faults occurring within the line length for several types of parallel line configurations. It is important to note that when the parallel line is de-energized and grounded at only one end, the protected line should be treated as a single-line configuration, as there is no zero-sequence mutually coupled current in the parallel line.

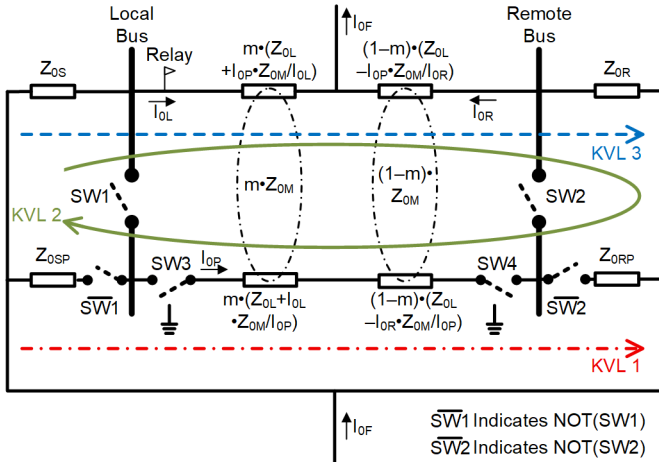


Fig. 28. Zero-sequence network for a fault at a distance  $m$  from the relay in a parallel line configuration.

Table III outlines the switch positions (SW1 through SW4) required to establish the zero-sequence network for a specific parallel line configuration. For the subsequent derivation, it is assumed that the zero-sequence impedance angles of the protected line and the parallel line are identical. Note that when the parallel lines differ in length, their arrangements can generally be categorized into one of the configurations shown in Fig. 28.

TABLE III  
SWITCH (SW1–SW4) POSITIONS IN ZERO-SEQUENCE NETWORK  
OF FIG. 28 FOR VARIOUS PARALLEL LINE CONFIGURATIONS

Parallel Line Configuration	SW1	SW2	SW3	SW4
Line Configuration 1: Parallel lines originating and terminating at a common bus	1	1	1	1
Line Configuration 2: Parallel lines originating from a common bus and terminating on separate buses	1	0	1	1
Line Configuration 3: Parallel lines originating from different buses and terminating at a common bus	0	1	1	1
Line Configuration 4: Parallel lines originating and terminating at separate buses	0	0	1	1
Line Configuration 5: Parallel line out of service and grounded at both ends	NA	NA	Grounded	Grounded
Line Configuration 6: Parallel line out of service and grounded at one end	NA	NA	Grounded	Not grounded

From Fig. 28, the expression for the parallel line zero-sequence current ( $I_{0P}$ ) can be derived using Kirchoff's voltage law (KVL).  $I_{0P}$  can be expressed as a function of local and remote terminal zero-sequence currents,  $I_{0L}$  and  $I_{0R}$ , respectively.

In Fig. 28, applying KVL around the loop labeled KVL 1, the expression of  $I_{0P}$  is obtained as shown in (15).

$$I_{0P} = aI_{0L} + bI_{0R} \quad (15)$$

where  $a$  and  $b$  are current distribution factors that are dependent on the zero-sequence network impedances and the fault location, as defined in Table IV.

Similarly, by applying KVL around the loop labeled KVL 2,  $I_{0P}$  can be expressed as shown in (16).

$$I_{0P} = cI_{0L} + dI_{0R} \quad (16)$$

where  $c$  and  $d$  are current distribution factors that are dependent on the zero-sequence network impedances and the fault location, as defined in Table IV.

Furthermore, the total zero-sequence fault current is written as shown in (17).

$$I_{0F} = I_{0L} + I_{0R} \quad (17)$$

Solving (15) through (17) results in (18).

$$\arg\left(\frac{I_{0F}}{I_{0L}}\right) = \arg\left(\frac{d-b+a-c}{d-b}\right) \quad (18)$$

Equation (18) represents the expression for zero-sequence tilt angle compensation in parallel line configurations. This equation demonstrates that the tilt angle compensation is a function of the zero-sequence parameters and the fault location. Importantly, it confirms that the tilt angle is independent of the zero-sequence current in the parallel line.

Let us consider a case of parallel transmission lines, as illustrated in Fig. 29, to evaluate the worst-case tilt angle for a zero-sequence current-polarized reactance element. The system depicted in Fig. 29 represents a practical scenario where the network is not perfectly homogeneous, as reflected by different zero-sequence impedance angles.

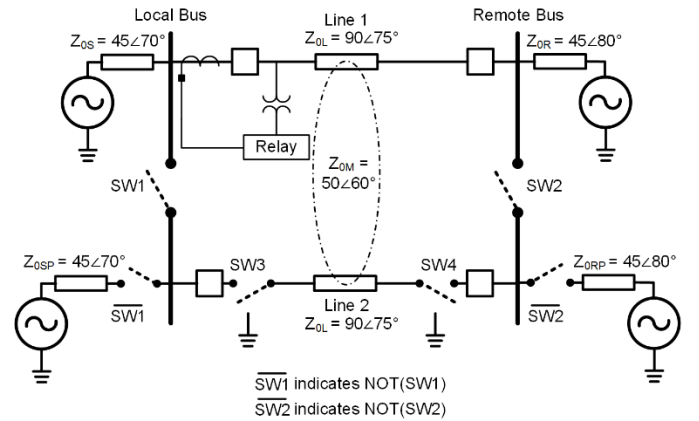


Fig. 29. Network representing various parallel line configurations.

TABLE IV

LOCAL AND REMOTE ZERO-SEQUENCE CURRENT DISTRIBUTION FACTORS TO DETERMINE PARALLEL LINE ZERO-SEQUENCE CURRENT USING (15) AND (16)

Parallel Line Configuration	a	b	c	d
Line Configuration 1: Parallel lines originating and terminating at a common bus	$-\left[\frac{m \cdot Z_{0M} + Z_{0S}}{Z_{0S} + Z_{0L} + Z_{0R}}\right]$	$\left[\frac{(1-m) \cdot Z_{0M} + Z_{0R}}{Z_{0S} + Z_{0L} + Z_{0R}}\right]$	m	$-(1-m)$
Line Configuration 2: Parallel lines originating from a common bus and terminating on separate buses	$-\left[\frac{m \cdot Z_{0M} + Z_{0S}}{Z_{0S} + Z_{0L} + Z_{0RP}}\right]$	$\left[\frac{(1-m) \cdot Z_{0M}}{Z_{0S} + Z_{0L} + Z_{0RP}}\right]$	$\left[\frac{m \cdot (Z_{0L} - Z_{0M})}{Z_{0L} - Z_{0M} + Z_{0RP}}\right]$	$-\left[\frac{(Z_{0L} - Z_{0M})(1-m) + Z_{0R}}{Z_{0L} - Z_{0M} + Z_{0RP}}\right]$
Line Configuration 3: Parallel lines originating from different buses and terminating at a common bus	$-\left[\frac{m \cdot Z_{0M}}{Z_{0SP} + Z_{0L} + Z_{0R}}\right]$	$\left[\frac{(1-m) \cdot Z_{0M} + Z_{0RP}}{Z_{0SP} + Z_{0L} + Z_{0R}}\right]$	$\left[\frac{m \cdot (Z_{0L} - Z_{0M}) + Z_{0S}}{Z_{0L} - Z_{0M} + Z_{0SP}}\right]$	$-\left[\frac{(1-m)(Z_{0L} - Z_{0M})}{Z_{0L} - Z_{0M} + Z_{0SP}}\right]$
Line Configuration 4: Parallel lines originating and terminating at separate buses	$-\left[\frac{m \cdot Z_{0M}}{Z_{0SP} + Z_{0L} + Z_{0RP}}\right]$	$\left[\frac{(1-m) \cdot Z_{0M}}{Z_{0SP} + Z_{0L} + Z_{0RP}}\right]$	$\left[\frac{m(Z_{0L} - Z_{0M}) + Z_{0S}}{Z_{0L} - Z_{0M} + Z_{0SP} + Z_{0RP}}\right]$	$-\left[\frac{(1-m)(Z_{0L} - Z_{0M}) + Z_{0R}}{Z_{0L} - Z_{0M} + Z_{0SP} + Z_{0RP}}\right]$
Line Configuration 5: Parallel line out of service and grounded at both ends	$-\left[\frac{m \cdot Z_{0M}}{Z_{0L}}\right]$	$\left[\frac{(1-m) \cdot Z_{0M}}{Z_{0L}}\right]$	$m + \frac{Z_{0S}}{Z_{0L} - Z_{0M}}$	$m - \left[\frac{(Z_{0L} - Z_{0M} + Z_{0R})}{Z_{0L} - Z_{0M}}\right]$

Fig. 30 presents the zero-sequence tilt angle, calculated using (18) for the system shown in Fig. 29. The current distribution factors a, b, c, and d for all possible parallel line configurations are obtained from Table IV. It is important to note that when the parallel line is de-energized and grounded at only one end, the protected line is considered as a single line. As such, the tilt angle is determined using the zero-sequence equivalent of (11).

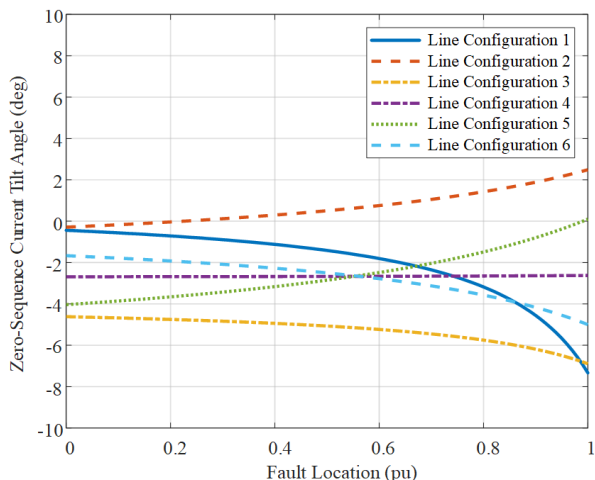


Fig. 30. Zero-sequence current polarization tilt angle along the length of the line for several parallel line configurations, which are outlined in Table III.

As shown in the plots of Fig. 30, the worst-case tilt angle across all configurations is  $-7$  degrees.

This example illustrates that even in practical systems, where the zero-sequence network is not perfectly homogeneous, a default tilt angle of  $-7$  degrees is generally sufficient for zero-sequence current polarization. However, it is still recommended to obtain the worst-case tilt angle for the specific system under consideration.

## IX. REFERENCES

- [1] *Directional Ground Distance Relay: Type GCXG51A11 & Up*, GEI-98339E.
- [2] G. Ziegler, *Numerical Distance Protection: Principles and Applications*, 2nd ed., Publicis Corporate Publishing, Erlangen, Germany, 2006.
- [3] W. Z. Tyska, "Polarization of Ground Distance Relays," proceedings of the 13th Annual Western Protective Relay Conference, Spokane, WA, October 1986.
- [4] J. B. Roberts, A. Guzmán, and E. O. Schweitzer, III, "Z = V/I Does Not Make a Distance Relay," proceedings of the 20th Annual Western Protective Relay Conference, Spokane, WA, October 1993.
- [5] *SEL-321, -1 Relay: Phase and Ground Distance Relay Directional Overcurrent Relay Fault Locator Instruction Manual*. Available: selinc.com.
- [6] B. Kasztenny, "Distance Elements for Line Protection Applications Near Unconventional Sources," proceedings of the 75th Annual Conference for Protective Relay Engineers, College Station, TX, March 2022.
- [7] F. Calero, "Mutual Impedance in Parallel Lines – Protective Relaying and Fault Location Considerations," proceedings of the 34th Annual Western Protective Relay Conference, Spokane, WA, October 2007.
- [8] D. A. Tziouvaras, H. J. Altuve, and F. Calero, "Protecting Mutually Coupled Transmission Lines: Challenges and Solutions," proceedings of the 67th Annual Conference for Protective Relay Engineers, College Station, TX, March 2014.
- [9] J. Roberts and A. Guzmán, "Directional Element Design and Evaluation," proceedings of the 21st Annual Western Protective Relay Conference, Spokane, WA, October 1994.
- [10] E. H. Gove and E. A. Taylor, "A Practical Remedy for Zero Sequence Reversal," proceedings of the 16th Annual Western Protective Relay Conference, Spokane, WA, October 1989.
- [11] *SEL-421-4, -5 Protection, Automation, and Control System Instruction Manual*. Available: selinc.com.
- [12] K. Dase, A. Guzmán, S. Chase, and B. Smyth, "Applying Dependable and Secure Protection With Quadrilateral Distance Elements," 77th Annual Conference for Protective Relay Engineers, College Station, TX, March 2024.
- [13] M. Nagpal and C. Henville, "BC Hydro Protection Interconnection Practices for Sources With Inverter or Converter Interface," proceedings of the 45th Annual Western Protective Relay Conference, Spokane, WA, October 2018.

- [14] M. Bini, R. Abboud, P. Lima, and F. Lollo, "Challenges and Solutions in the Protection of Transmission Lines Connecting Nonconventional Power Sources," proceedings of the 48th Annual Western Protective Relay Conference, Spokane, WA, October 2021.

## X. BIOGRAPHIES

**Kanchanrao Dase** earned his Bachelor of Engineering degree in Electrical Engineering from Sardar Patel College of Engineering, University of Mumbai, India, in 2009. He completed his Master of Science degree in Electrical Engineering from Michigan Technological University in 2015. From 2009 to 2014, he worked as a manager at Reliance Infrastructure Limited, with a substation engineering and commissioning profile. He is currently a senior engineer in the Research and Development division at Schweitzer Engineering Laboratories, Inc. (SEL). His interests include power system protection, substation automation, and fault locating. He is a senior IEEE member and a registered Professional Engineer (PE) in Washington State. He has authored several technical papers and currently holds six patents.

**Kale McCarthy** received his Bachelor of Science degree in electrical engineering with highest honors from Montana Technological University in 2023. He joined Schweitzer Engineering Laboratories, Inc. (SEL) as an intern in 2022 and was then hired as a product engineer in 2023 in the transmission department. In addition to working at SEL, Kale joined Montana Tech in 2025 as an affiliate professor, where he teaches courses in power system protection. He is an active IEEE member.

**Muhammad Ashraf** is a senior protection application engineer in the Sales and Customer Service division of Schweitzer Engineering Laboratories, Inc. (SEL). He received his Bachelor of Science degree in Electrical Engineering in 2008 from the University of Engineering and Technology (UET), Lahore, Pakistan. He is a member of IEEE and has over 17 years of experience in power system protection applications, design, and testing and commissioning. He worked as a system protection engineer at the national transmission utility company in Pakistan, prior to joining SEL in 2015.

**Armando Guzmán** (M '95, SM '01) received his BSEE with honors from Guadalajara Autonomous University (UAG), Mexico. He received a diploma in fiber-optics engineering from Monterrey Institute of Technology and Advanced Studies (ITESM), Mexico, and his Master of Science and PhD in electrical engineering and Master of Engineering in computer engineering from the University of Idaho. He served as regional supervisor of the Protection Department in the western transmission region of the Federal Electricity Commission (the electrical utility company of Mexico) in Guadalajara, Mexico, for 13 years. He lectured at UAG and the University of Idaho on power system protection and power system stability. Since 1993, he has been with Schweitzer Engineering Laboratories, Inc. (SEL) in Pullman, Washington, where he is a distinguished engineer. He holds numerous patents in power system protection, fault locating, and monitoring. He is a senior member of IEEE.